ELSEVIER

Physica A 292 (2001) 87–101

PHYSICA A

www.elsevier.com/locate/physa

Computer simulation of water–ice transition in hydrophobic nanopores

Jan Slovák[a], Hideki Tanaka[b,*], Kenichiro Koga[c], Xiao C. Zeng[d]

[a] *E. Hata Laboratory of Thermodynamics, Institute of Chemical Process Fundamentals, Acad. Sci., 165 02 Prague 6, Czech Republic*

[b] *Department of Chemistry, Faculty of Science, Okayama University, 3-1-1 Tsushima-naka, Okayama 700-8530 Japan*

[c] *Department of Chemistry, Fukuoka University of Education, Fukuoka 811-4192, Japan*

[d] *Department of Chemistry and Center for Materials & Analysis, University of Nebraska, Lincoln, Nebraska 68588, USA*

Received 23 October 2000

Abstract

A series of molecular dynamics simulations is performed in order to examine in more detail the results of a previous simulation which shows that a thin film of water, when confined in a hydrophobic nanopore, freezes into a bilayer ice crystal composed of two layers of hexagonal rings. Three simulations are carried out and each starts with a different initial configuration but has the same number of molecules and the area density. Using a previously introduced solid-like cluster definition, we monitor the dynamic process of crystallization. We find that only in one case the confined water completely freezes into perfect bilayer ice whereas in other two cases, an imperfect crystalline structure consisting of hexagons of slightly different shapes is observed and this imperfection apparently hinders the growth of perfect bilayer crystal. After adjusting the area density to match spatial arrangements of molecules, the latter two systems are able to crystallize completely. As a result, we obtain three forms of bilayer crystal differing in the area density and hexagonal rings alignment. Further analyses of these bilayer crystals provide more insightful explanation on the influence of the boundary condition and the simulation-cell size on the diversity of possible crystallographic structures.

PACS: 64.70.Ja; 61.20.Ja

Keywords: Water; Nanopore; Nucleation; Bilayer ice

* Corresponding author. Fax: +81-86-251-8497.
E-mail address: htanakaa@cc.okayama-u.ac.jp (H. Tanaka).

0378-4371/01/$ - see front matter
PII: S0378-4371(00)00579-3

1. Introduction

Nanoscale systems such as nanoclusters, nanowires, and nanoplates are currently attracting considerable attention because of their great potential to make important contribution in nanotechnology. The design and preparation of nanostructured materials including, for example, quantum dots, single electron transistors [1], thin layered microstructures, reagent films for biosensors, and devices for optoelectronics [2], require knowledge and control of nanoarchitectures from the very early stages of self-organization. This requirement includes the control of nucleation growth, morphology and dissolution of crystals.

The large surface area-to-volume ratio of nanoscale materials also provides an opportunity for fundamental studies of the effects of nanoscale size and surface interactions on the phase transitions. In this paper, we focus on the phase transition of a thin film of water confined in hydrophobic slit nanopores by molecular dynamics (MD) computer-simulation method. Tools of computer simulation have been proved to be very useful to obtain deeper insight into the complex behavior of confined fluids. In particular, computer simulations for water enable us to understand on the molecular level the co-operativity of hydrogen bonding, solvation, and hydrogen bond network rearrangement dynamics. Moreover, computer simulations also allow us to study metastable states of supercooled water (like low- and high-density amorphous [3]) under conditions that are either expensive or difficult to achieve in laboratory experiments. Some new phases and new features of metastable water have been found from computer simulations.

Recently, we performed an MD simulation of liquid–solid phase transition of a confined TIP4P water [4,5] in a narrow slit composed of two parallel hydrophobic walls [6,7]. The width of the slit is about one nanometer, just enough to accommodate two layers of water molecules at certain density. When lowering the temperature of the system at a fixed normal pressure, the water undergoes a phase transition from a liquid to a solid. It is found [6] that the resulting solid phase is a crystalline ice, namely, a bilayer ice crystal. The structure of the bilayer ice resembles none of the known structures of the ice polymorphs. Nevertheless, the ice crystal still retains basic features of bulk ices. For example, every molecule is hydrogen bonded to four-nearest-neighbor molecules. Each layer of ice is composed of slightly distorted hexagonal rings (but still very flat compared to those in ice Ih or Ic), and the two layers are completely in registry.

The original simulations were performed at a normal pressure of 50, 150 MPa and 1 GPa, respectively, and in all three cases, the resulting solid phase has exactly the same bilayer crystalline structure. Computationally, it is more difficult and time consuming to detect the phase transition at lower normal pressures because the transition temperature would be much lowered with decreasing the pressure. It is also found that once the bilayer ice is formed, it will remain stable even after removing the two confining walls, at least within the timescale of computer simulation.

In a previous study [7], effects of the simulation cell size and those of the initial conditions were not investigated systematically. The aim of this work is twofold: to examine effects of the initial configuration on the time evolution of the crystal phase and to elucidate the extent to which the size of simulation cell and the periodic boundary conditions affect the process of crystallization and the shape of final crystal.

2. Simulation and structure analysis

2.1. Simulation

We perform three MD simulations of water confined within two plane parallel structureless walls, at fixed temperature ($T=253$ K) and fixed normal pressure ($P_z=1$ GPa). The water molecules interact with each other via TIP4P potential and with the two walls via the 9-3 Lennard–Jones potential. The long-range water–water potential is smoothly truncated at 8.665 Å. The simulation cell is a rectangular prism with lateral dimensions $L_x = 65.01$ Å and $L_y = 65.684$ Å; thus, keeping the area density $\rho_A = N/A = N/L_xL_y$ fixed. The confined system consists of a fixed number of water molecules $N = 896$. The distance between the walls, L_z, is about 1 nm. Periodic boundary conditions are imposed in the x and y directions. To generate distinct initial configurations, we use configurations stored during a simulation at $T = 257$ K at which the system is well equilibrated and never shows a tendency towards freezing (at least not on computer simulation time-scale). We select three distinct configurations in the course of simulation, which are separated by a time lag of about 2 ns. Next, we assign new velocities to the molecules according to Boltzmann distribution and let the system develop into equilibrium state at the same temperature. Then, the temperature is lowered to 253 K and the system is let to reach a new equilibrium state again. In this way, we generate three configurations that will be used as the starting configuration for MD simulations.

It has been shown [8,9] that the induction time and the size of critical nucleus depend strongly on the number of particles of the system. For a three-dimensional Lennard–Jones system, Swope and Andersen concluded that at least 15 000 atoms are required to describe correctly the kinetics of crystal growth from a melt. For the quasi-two-dimensional confined water, it is unclear how large the system size should be in order to remove artifacts due to the finite system size and the periodic boundary condition. Other than effects of the system size, the rectangular shape of the simulation cell would enforce a particular arrangement of molecules and thus would also play a certain role in crystallization.

2.2. Structure analysis

Every instantaneous configuration generated in the MD simulation entails a vibrational displacement from a local minimum of the potential energy hypersurface. The

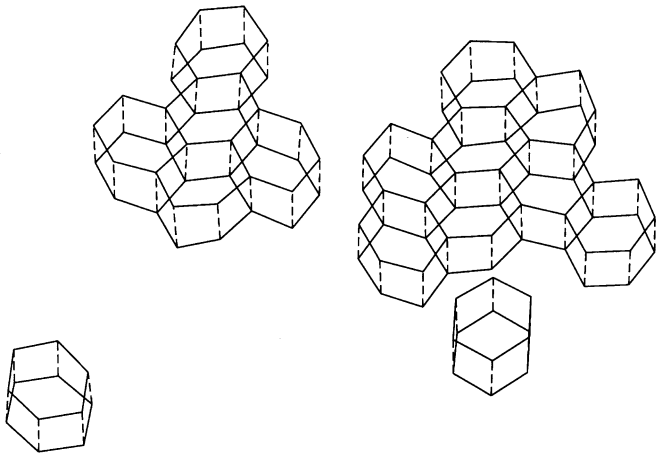

Fig. 1. A typical example of spatial arrangement of water molecules in the clusters based on our cluster definition. The solid lines depict the hydrogen bonds in each layer, the dashed ones are HB connecting molecules in upper and lower layers.

potential energy of an instantaneous configuration (hereafter called I-structure) has two contributions: the potential energy of the minimum-energy structure, and the thermal excitations. The minimum-energy structures are referred to as quenched structures (Q-structures [10–12]) and can be obtained using the steepest descent method. The Q-structures provide useful information about the structure in configuration space and the geometry of molecular arrangement in solid state.

We characterize the solid state and solid-like regions based on the appearance of the domain of hexagonal cells. The hexagonal cell is considered to be an elementary unit of the bilayer crystalline structure. It is composed of a pair of coupled hexagonal rings of hydrogen bonded molecules, i.e., a hexagonal ring in one layer with its counterpart in another. A single hexagonal cell is the smallest unit having solid-like features and we will regard it as the smallest embryo of the solid phase. The crystal grows via attaching more and more hexagonal cells. We call the two hexagonal cells *neighboring* if they share four molecules and *connected* if there is a chain of *neighboring* cells. Thus, a solid cluster is defined as a maximally connected set of hexagonal cells. Fig. 1 shows an example of a configuration during freezing process, which contains four clusters of sizes 8, 5, 1. With this definition of solid cluster, we need not impose any restrictions on the same shape of hexagons and their mutual arrangement.

3. Results and discussion

In a previous study, we performed an MD simulation for a system of 896 water molecules confined to a hydrophobic slit at $T = 253$ K [7]. Here, we perform two additional MD simulations at the same temperature and with the same number of molecules but starting from different initial configurations of molecules. For the sake of analysis,

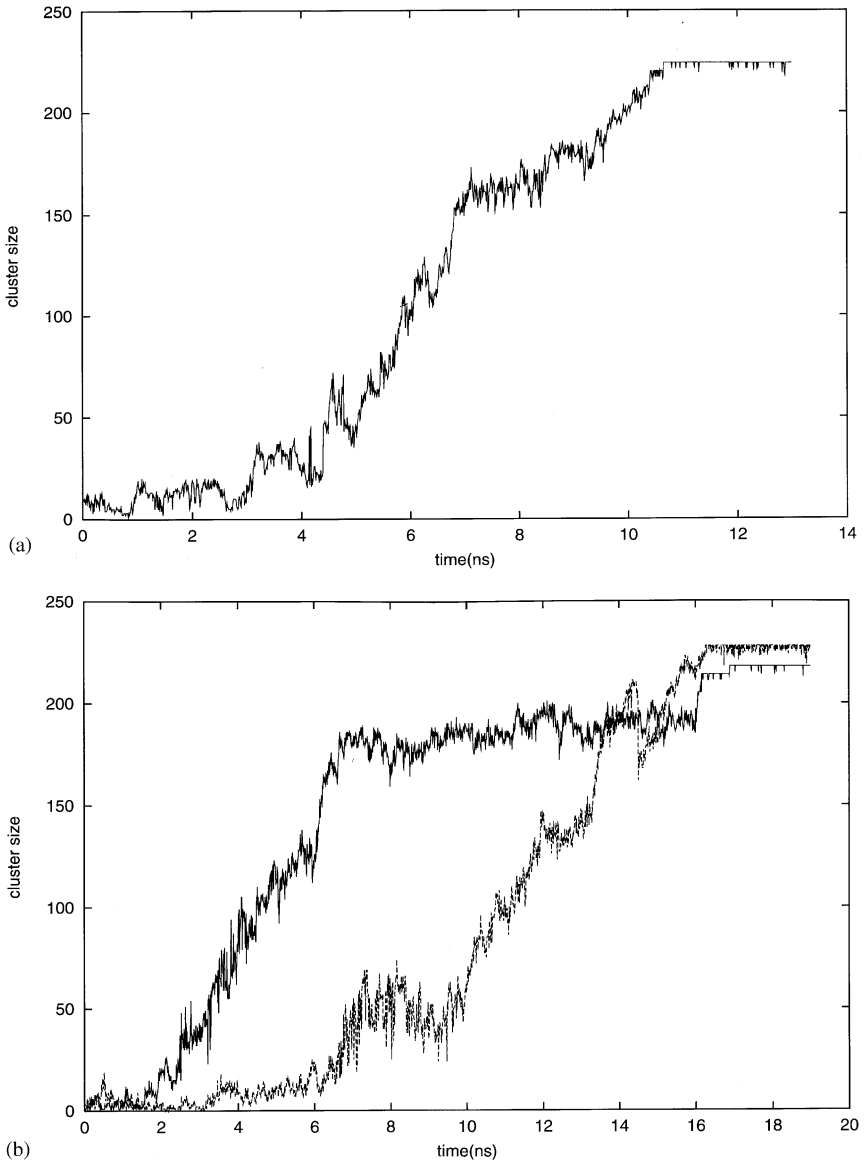

Fig. 2. The maximum cluster size as a function of time for simulation S1 (a) and simulations S2 (solid line) and S3 (dashed line) (b).

we store every thousandth configuration with the time step being 5×10^{-16} s. These instantaneous configurations are subsequently quenched and the resulting Q-structures are used for structural analysis. Hereafter, we will refer to our three simulations as S1, S2 and S3.

During the simulations, we monitor the size distribution of solid-like clusters. Fig. 2 shows the time evolution of the maximal cluster size for the three independent

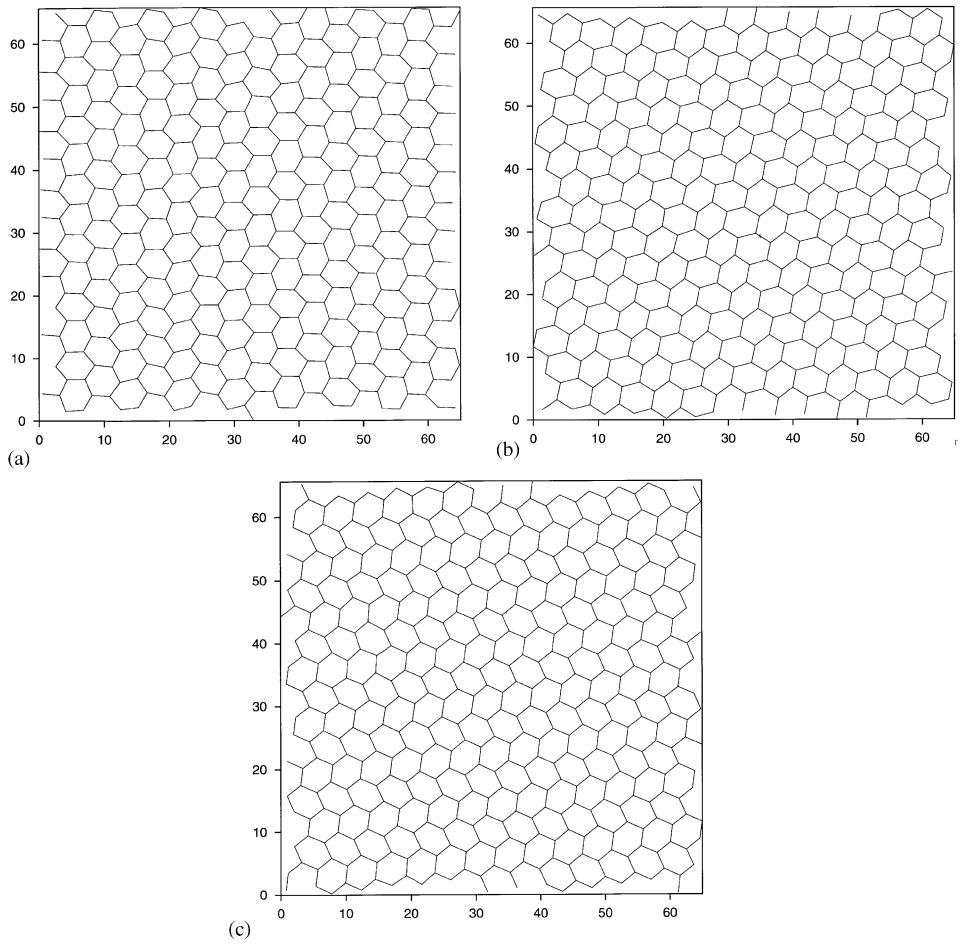

Fig. 3. The final crystalline structures for simulation S1 (a), simulation S2 (b) and simulation S3 (c) (xy projection).

simulations. Fig. 2(a) depicts the result of S1 [7]. The confined water gradually freezes and finally forms a crystal composed of 224 hexagonal cells. The crystal appears at about $t = 10.5$ ns and apparently is stable during the next 2.5 ns, only occasionally breaking up few of the hydrogen bonds. A snapshot of molecular arrangement in one of the final configurations is shown in Fig. 3(a). The crystallization processes in S2 and S3 are found to be quite different from that in S1. We can see in Fig. 2(b) that the solid embryo in S2 grows very quickly during the first 6–7 ns but it never ends up in a complete crystal within the simulation time scale. A closer look into the configurations reveals that the hexagonal cells line up in slightly different directions compared to those in S1 and have slightly different shapes: the hexagons do not have exactly the same inner angles as those in S1. This yields heterogeneity in spatial distribution

of molecules. In fact, there is a liquid-like hole in the solid-like system, which consumes too many molecules to generate the missing hexagonal cells in the spot. Thus, formation of a perfect bilayer crystal cannot be completed unless some major structural rearrangements take place in the solid region. However, the hole is too small to cause serious damage in the already formed crystalline structure such as complete disintegration of solid region or change in the alignment of hexagons. Once the rows of hexagonal cells are connected over the simulation cell, it is very difficult to break this connection. If certain number of molecules are removed from the liquid-like hole, the process of crystallization would complete successfully. In the case of S2, we observed a crystal composed of 218 hexagonal cells (872 molecules) which seems to be perfectly stable after its formation. In the case of S3, a liquid-like hole appears again but it comprises less molecules than those needed to form the missing hexagonal cells. Thus, to complete the crystallization, additional molecules should be put into the hole. Adding is technically more difficult than removing molecules and we will not come into too much details. After adding certain number of molecules, we obtain a crystal composed of 228 hexagonal cells (912 molecules) which again is very stable in the course of the simulation.

Fig. 2(b) shows the time dependence of maximal cluster size in S2 and S3. The number of molecules is adjusted at $t=16$ ns for S2 (from 896 to 872) and at $t=14.5$ ns for S3 (from 896 to 912). We observe quite a sharp decrease in the maximal cluster size at $t=14.5$ ns for S3. It depends on the way how the additional molecules are put into the system. In S2 it is possible to remove some molecules from the hole and thus the maximal cluster size remains the same whereas in S3 we have to 'blow up' the hole, that is, to reduce the already frozen region. In this way, we are able to change the maximal cluster size. Fig. 3(b) and (c) show the xy-projections of the final crystals. Fig. 4 is given to provide a better picture of how the molecules are arranged. The picture corresponds to S2 but looks nearly same as those in S1 and S3.

One may ask the way we handle the system size because it is unnatural to suddenly change the number of particles in the system. We remark that the main purpose to employ this method is to be able to prepare various solid states and then analyze them. We find that at a certain point of simulation the system will not form a regular crystal within the time scale of simulation. Once the freezing process is stuck, adjusting the number of molecules and restarting the simulations offers a quick way, though unnatural, to induce formation of regular crystals. We can show that the crystals thus obtained are indeed stable so that their existence is justified despite the use of unnatural means.

Another question to be asked is: do the molecules align in a certain way from the very beginning of a simulation? The answer is very unlikely. Then what is the decisive point in a simulation at which the freezing takes place? It appears that the boundary condition play a very important role in crystallization and this somewhat dictates the crystalline forms that fit into the simulation cell. If the surface area of the simulation cell is not fixed, would the results be different?, e.g., using an NPT ensemble? Would the results be different if different boundary conditions are chosen? To answer

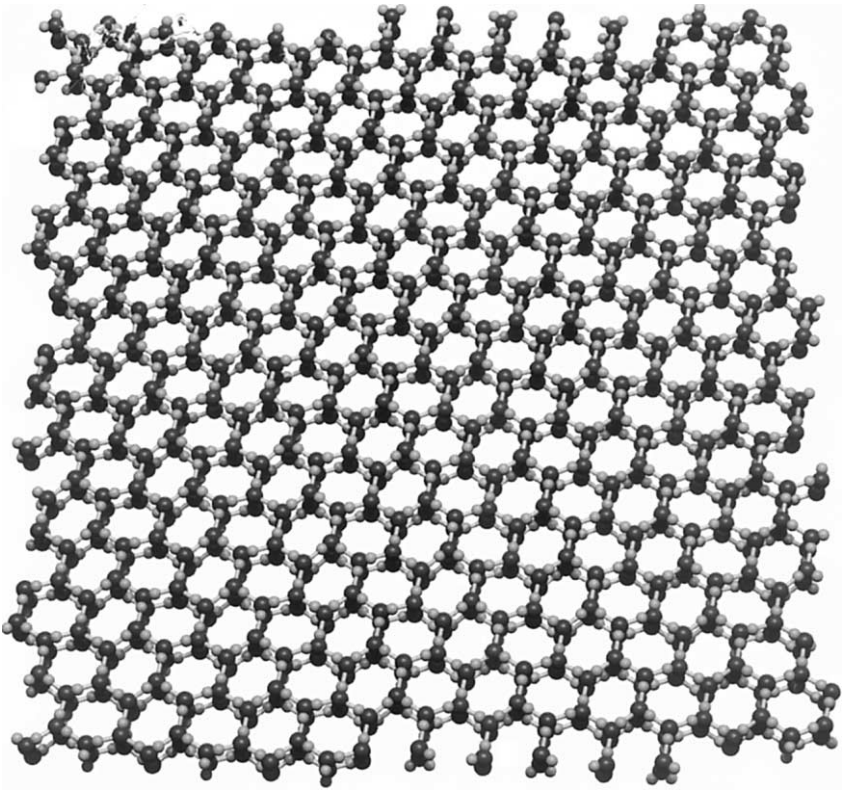

Fig. 4. A typical example of spatial arrangement of molecules in a final configuration in simulation S2.

these questions, we have to conduct a more detailed structural analysis of the resulting crystals.

First, let us recall the bilayer ice rules formulated previously [6]. Note that in the TIP4P bilayer ice, each hexagon has a side length (O–O separation) of 2.73 ± 0.02 Å and three different angles: $\alpha = 108^\circ$, $\beta = 117.5^\circ$, and $\gamma = 134.5^\circ$ (all within the error bar $\pm 2^\circ$). The first ice rule is that the HOH angle is never superposed over the β and γ angles. The second rule is that when one OH bond of a water molecule is normal to the hexagonal lattice plane, the other OH bond can point only along a direction adjacent to the α angle edges. All the hexagons are congruent but with two different chiralities A and B. The hexagons with the same chirality always line up in a row. The bilayer crystal is composed of alternating rows of A's and B's. Under the two bilayer ice rules, the total number of possible arrangements of molecular orientations can be counted exactly, which is $W^{\text{bilayer}} = 2^{N/4}$. Thus, the residual entropy of the bilayer ice crystal is given by

$$S^{\text{bilayer}} = k_{\text{B}} \text{ In } W^{\text{bilayer}} = k_{\text{B}} \ln 2^{N/4} , \tag{1}$$

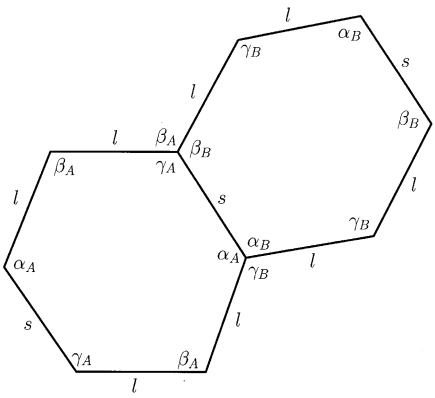

Fig. 5. Geometry of the hexagonal rings in the bilayer ice crystal.

Table 1
Arrangement and geometry of hexagonal rings in a crystal. *A* and *B* denote two types of hexagons which generally occur in the resulting structure. *l* stands for longer sides and *s* for shorter sides of hexagons

Simulation	α_A	β_A	γ_A	α_B	β_B	γ_B	*l*	*s*
I	117.5	108.5	134.5	108.0	117.5	134.5	2.73	2.73
II	112.5	110.0	137.5	115.0	112.5	132.5	2.78	2.75
III	115.5	105.5	139.0	107.5	115.5	137.0	2.72	2.72

where k_B is Boltzmann constant. Indeed, we find these rules also hold for the bilayer crystals generated in S2 and S3 when the crystallization completes. In all three cases, the crystals is composed of alternating rows of type-*A* hexagons and type-*B* hexagons. The two hexagons differ not only in chirality but also in the inner angles and side lengths. The direction of the rows is also different. But there are always only two types of hexagons. Fig. 5 schematically shows the geometry of the two hexagons. The numerical values of inner angles and side lengths are given in Table 1. Another way to state the two bilayer ice rules can be as follows. (1) The HOH angle can only be superposed over angles β_A, α_B; (2) when one OH bond of water molecule is normal to the hexagonal lattice plane, the other OH bond can point only along a direction adjacent to the β_A and α_B angle edges. In the simulations, we actually observed some exceptions from the bilayer ice rules. Since there are very few of them (less than 5 defects in the whole crystal in S1 and S2 and no defects in S3), we consider these exceptions non-essential. The residual entropy can be estimated with high precision using Eq. (1).

Note also that not every hexagonal ring has the exact shape as depicted in Fig. 5, which is averaged over large number of configurations. All the angles given in Table 1 are within error $\pm 2^\circ$ and the side lengths within error ± 0.02 Å. The distribution of inner angles of hexagons for all the three structures is shown in Fig. 6 and the comparison of O–O distance distributions is shown in Fig. 7. Figs. 8 and 9 show the binding-energy distributions and pair interaction-energy distribution. They

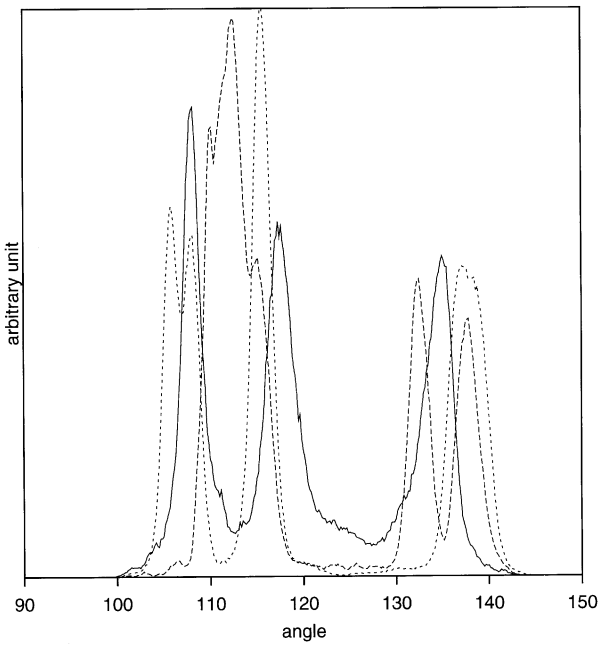

Fig. 6. Comparison of hexagon inner-angle distributions in simulation S1 (solid line), S2 (dashed line) and S3 (dotted line).

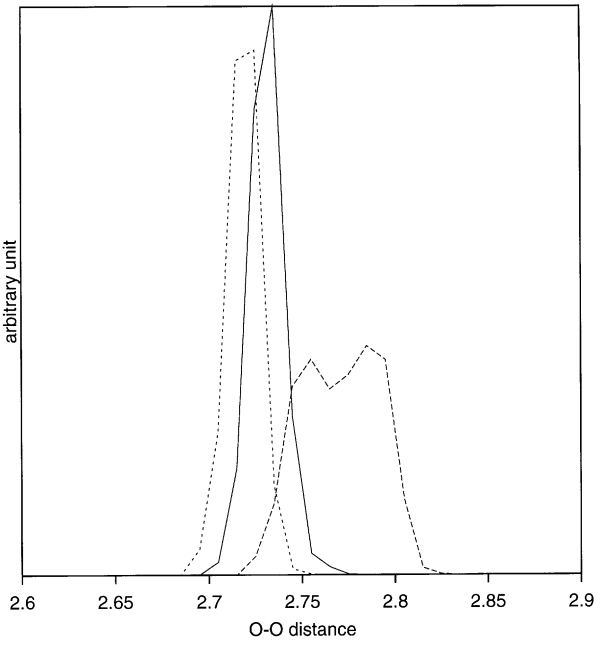

Fig. 7. Comparison of O–O distance distribution in simulation S1 (solid line), S2 (dashed line) and S3 (dotted line).

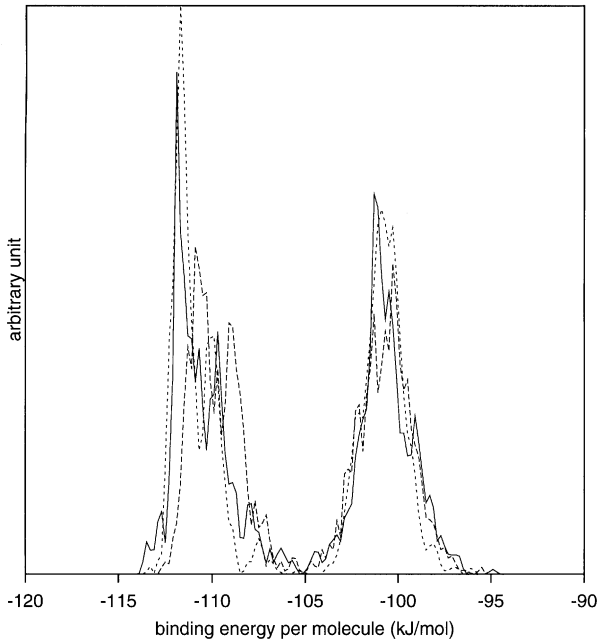

Fig. 8. Comparison of the binding energy distributions in simulation S1 (solid line), S2 (dashed line) and S3 (dotted line).

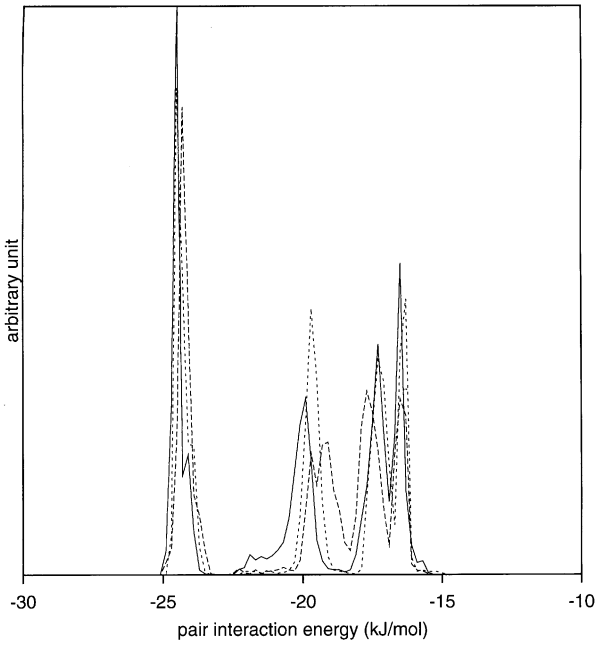

Fig. 9. Comparison of the pair interaction energy distributions in simulation S1 (solid line), S2 (dashed line) and S3 (dotted line).

are quite similar. The average potential energy per molecule is $E_1 = -52.79$ kJ/mol for S1, $E_2 = -52.59$ kJ/mol for S2, and $E_3 = -52.92$ kJ/mol for S3. Although both S1 and S2 crystals are more or less regular, the S1 crystal possesses more imperfections. Every two hexagons in a row of hexagonal cells are translationally invariant in S2, S3 crystals. This is not the case for S1 crystal, which can be clearly seen from Fig. 3(a).

We also found all three structures, once formed, seem to be very stable. It seems that there is certain flexibility in O–O–O angles of hydrogen bonded triplets, as well as in O–O distance of a pair of hydrogen bonded molecules. Potentially there are several possible directions in which rows of hexagons can be lined up. It would be an enormous task to classify all such structures but apparently there are many of them, each one differing in hexagonal shapes and even hydrogen bonded pair distances.

Our simulations indicate that for a given simulation-cell size, there are certain 'magic' numbers of molecules for which some special initial liquid configurations exist and will freeze into regular crystalline structure without any defects. There is a certain number of non-equivalent crystalline structures in the simulation cell of the given size. Increasing the size of simulation cell, the total number of crystalline structures that fit into the cell is expected to be larger. For illustration: If we increase the lateral dimensions of the simulation cell 2 times (i.e., the area 4 times), then by taking 4 replicas of the smaller cell we can immediately generate one crystalline structure in the larger cell. But not vice versa. In the larger cell, there are generally other crystalline structures which do not exist in the smaller one. If we increase significantly the size of simulation cell, the number of possible structures will increase but as for their hexagons, they will be closer in shape, so the different structures would show up mainly due to the different alignment of rows of hexagons.

Let us take a closer look at the early stages of crystallization. In the early stages of crystallization our analysis shows that the flexibility in hexagon angles is much higher than that in O–O distance. Fig. 10 gives an example of an early configuration in S2. The alignment of hexagonal cells in one part of a cluster resembles that in one of S1 crystal and in another part resembles that in one of S2 crystal. At $t = 6 - 7$ ns the embryo of crystal begins to look like a portion cut from the final crystal, i.e., at about this time the alignment of hexagonal rings is established. Are their shapes established at final stages as well? The angle analysis shows that even at the end of S2 and just before removing molecules from the system, there exist only two distinct angles in the distribution, which means that there appears only one type of hexagon with inner angles $\alpha = 111^\circ$, $\beta = 111^\circ$ and $\gamma = 138^\circ$. This distribution is a result of averaging, and actually all the peaks in the distribution are very broad and not all the hexagons have the same angles. There is quite a large portion of hexagons with all the three angles different. But the number of hexagons with $\alpha = \beta$ slightly prevails, which gives the broad peak around the value of 111°. On the other hand, at the end of regular S3 simulation, the angle distribution is exactly the same as that one of S1. The angle distributions become those depicted in Fig. 6 only after the number of molecules in the system is adjusted.

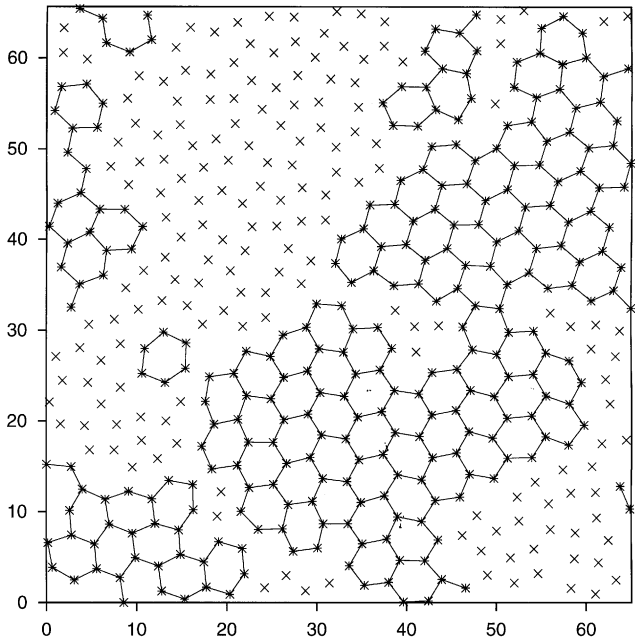

Fig. 10. An example of an intermediate state during the simulation S2 ($t = 4$ ns).

If we let a system crystallize at an arbitrary density, generally we will obtain a crystal with some defects. These defects can move around throughout the system, change their size, and interact with each other. But with the periodic boundary condition, they will never reach a boundary and travel out of the system. If a free boundary condition is employed, the defects could reach a boundary after certain time and take part in extending crystalline structure at the boundary after some movement.

Is that possible to reduce the influence of periodic boundary condition using some other simulation method? To what extent does that method be appropriate? Further studies are needed to answer these questions. However, we can make a few general comments here to elucidate the physics behind the simulations. Our system is inhomogenous so that instead of bulk pressure, in general, we need to consider stresses. We can still define the lateral pressure $P_x(=P_y) \equiv L_z^{-1}(\partial F/\partial A)_{NTL_z}$ and the normal pressure $P_z \equiv A^{-1}(\partial F/\partial L_z)_{NTA}$. Here, F is the Helmholtz free energy and A the surface area of the slit. The volume is then $V = AL_z$. In the case of a rectangular simulation cell, $A = L_x L_y$. Because of the strong system anisotropy, generally $P_x \neq P_z$. Note that in real experiments for the study of phase transition, one usually controls stresses. To mimic the real experiments, an NP_xP_zT simulation seems a better choice. In fact, the quantity playing the role of bulk pressure is P_x. This is because the free energy is extensive with respect to A, i.e.,

$$F(N, A, L_z, T) = Af(N/A, L_z, T) \tag{2}$$

but not with respect to L_z. This shows that P_x and A are quantities analogous to the bulk pressure and bulk volume for bulk system. In this work we use NAP_zT simulation. The constraints can be implemented in computer simulation but they are not very natural. More realistic constraints would partially reduce the problems associated with periodic boundary condition and small-system size, although P_x may be different from the bulk pressure in equilibrium with water between two walls.

4. Concluding remarks

A series of three MD simulations for a thin film of water confined to a hydrophobic slit is performed in order to examine the effects of the initial configurations on the evolution process of the crystal embryo and to study the influence of simulation cell size and periodic boundary conditions on crystallization process. Upon freezing the system forms a bilayer ice crystal composed of hexagonal cells. In general, two types of hexagonal cells are seen, each aligning in rows with different orientations. In one simulation, the system freezes completely while in other two simulations incomplete structures containing a liquid-like region show up. These regions contain less than 100 molecules, i.e., less than one-tenth of the total number (896 molecules) in the system. It is conceivable to make the system crystallize completely by altering the number of molecules in the system. Once formed, the incomplete crystals do not change significantly. The direction in which the rows of hexagonal cells line up also stays fixed mainly due to the cell shape and the periodic boundary condition.

The influence of periodic boundary condition on nucleation has been reported many times for systems with simple intermolecular interaction (e.g. [13–15]). It has been pointed out that for smaller systems, the observed rapid crystallization after some induction time is not related to the formation of critical nucleus but just an artifact of periodic boundary condition. For three-dimensional systems, the minimal system size to avoid the artifacts has been estimated to be about 15 000 particles. A main difference between our system and previously studied simple systems is that we do not have all the information about the bilayer crystalline structure in a quantitative fashion. For Lennard–Jones solid, it is well known that one possible crystalline structure is fcc so that one can clearly identify the defects in crystalline structure after the crystallization is completed. For bilayer ice, however, the inner angles of hexagons often differ marginally. A question naturally arises: Is the A type hexagon in S2 the 'right' one or the A type in S3 the 'right' one? Unless a very long simulation is performed for a large enough bilayer ice crystal with either free boundary condition or with periodic boundary condition, we do not know the exact values of inner hexagon angles. A detailed study of the nucleation and a reliable estimation of critical nucleus size must await a much larger scale simulation. The system size and shape to be employed also depend on the size of critical nucleus since the smaller the critical nucleus the less influence the cell size and shape would have.

Acknowledgements

HT and KK are supported by grants from JSPS and Ministry of Education and XCZ was supported by grants from NSF, ONR, and a fellowship from JSPS.

References

[1] A.P. Alivisatos, Science 271 (1996) 933.
[2] H. Rapaport, J. Phys. Chem. B 104 (2000) 1399.
[3] O. Mishima, H.E. Stanley, Nature 396 (1998) 329.
[4] W.L. Jorgensen, J. Chem. Phys. 77 (1982) 4156.
[5] W.L. Jorgensen, J. Chandrasekhar, J.D. Madura, R.W. Impey, M.L. Klein, J. Chem. Phys. 79 (1983) 926.
[6] K. Koga, X.C. Zeng, H. Tanaka, Phys. Rev. Lett. 79 (1997) 5262.
[7] J. Slovák, K. Koga, H. Tanaka, X.C. Zeng, Phys. Rev. E 60 (1999) 5833.
[8] J.D. Honeycutt, H.C. Andersen, J. Phys. Chem. 90 (1986) 1585.
[9] W.C. Swope, H.C. Andersen, Phys. Rev. B 41 (1990) 7042.
[10] F.H. Stillinger, T.A. Weber, J. Phys. Chem. 87 (1983) 2833.
[11] F.H. Stillinger, T.A. Weber, Science 225 (1984) 983.
[12] I. Ohmine, H. Tanaka, P.G. Wolynes, J. Chem. Phys. 89 (1988) 5852.
[13] B.J. Alder, T.E. Wainwrigt, J. Chem. Phys. 33 (1960) 1439.
[14] M.J. Mandell, J.P. McTague, J. Chem. Phys. 66 (1977) 3070.
[15] J.D. Honeycutt, H.C. Andersen, Chem. Phys. Lett. 108 (1984) 535.